Progress In Electromagnetics Research M, Vol. 61, 159–167, 2017

A Quad-Band CPW Fed Slot Antenna Array for LTE and WiMAX Applications

Manzoor Elahi[1], Rizwan Khan[2, *], Azremi A. Al-hadi[2], Saeeda Usman[1], Ping Jack Soh[2], and Habibullah Khan[1]

Abstract—In this work, a quad-band omnidirectional slot antenna array is proposed. The structure consists of two closely-spaced radiating elements fed using coplanar waveguide (CPW) line. This combined structure is then integrated in a tapered slot etched on the antenna to enable operation in four frequency bands (0.8, 1.8, 2.6 and 3.45 GHz) for LTE and WiMAX applications with at least −10 dB of reflection coefficient. The antenna dimensional parameters are also studied to understand its behaviour and effects on its performance in facilitating the optimization process. Measurements of the fabricated antenna on a low-cost FR4 substrate validate its operation centred at 0.845 (from 0.77 to 0.92 GHz), 1.745 (from 1.59 to 1.9 GHz), 2.655 (2.59 to 2.72 GHz) and 3.49 GHz (from 3.28 to 3.7 GHz). Meanwhile, simulated and measured radiation patterns of the proposed antenna in all bands agree well and are omnidirectional, making is suitable for application in mobile terminals.

1. INTRODUCTION

Over the last two decades, developments in wireless communication systems have made it possible to share a huge amount of information by broadcasting digital video information to mobile handsets for consumers and other public safety radio systems such as police, fire-fighters and emergency medical personnel. Current mobile terminals are required to support various frequency bands, whereas the use of multiple single-band antennas will be costly in terms of space, which is already limited in such devices. The recent introduction of LTE (Long Term Evolution) systems to enable high speed data transfer for video and multimedia applications has increased the demands of such multiband antennas with minimal weight and cost [1, 2].

Integrated antennas such as microstrip and slot antennas are advantageous as they are typically small in size, can be easily integrated with electronic circuitry and have low cost [3]. Printed slot antennas are unique relative to microstrip antennas as they generally provide wider bandwidth, ease of impedance matching, and their radiation can be designed to be either bidirectional [4, 5] or unidirectional [6]. The simple uni-planar configuration also makes them suitable for various applications [7–9]. Slot antennas can be fed using microstrip or coplanar waveguide (CPW) lines. CPW feed offers low radiation losses, less dispersion, and characteristic impedance control over microstrip line feeds [10–13]. Such a feeding method can also be easily integrated with series and shunt devices without the need for via-holes on the ground plane, which introduces additional parasitic inductance and degrades antenna performance at higher frequencies.

Many CPW-fed multiband antenna designs have been proposed [14–24, 26–28], including several operating below 2 GHz, and such topology has also been widely used to design UWB antennas. While

Received 28 August 2017, Accepted 14 October 2017, Scheduled 27 October 2017

* Corresponding author: Rizwan Khan (rizwanjadoon@ciit.net.pk).

[1] Department of Electrical Engineering, COMSATS Institute of Information Technology, Sahiwal, Pakistan. [2] Advanced Communication Engineering (ACE) Centre of Excellence, School of Computer and Communication Engineering, Universiti Malaysia Perlis, Kangar, Perlis 01000, Malaysia.

various approaches have been adopted to achieve multi-band antenna operation for planar antennas, a widely used method to achieve this is to introduce slots in the ground plane or in the radiating element [14–22]. Using this method, different operating frequencies and their bandwidth are introduced by proper design and placement of these slots on the antenna. However, as the placement of multiple slots easily modifies the surface currents on the antenna, the design procedure needs to be performed systematically to ensure the achievement of the desired frequencies and bandwidths. An antenna based on a bow-tie monopole presented in [23] uses the top-loading technique to enable multi-band resonance in the structure. Meanwhile, researchers in [24, 25] introduced parasitic elements which are shortened with the ground plane to facilitate the generation of resonant modes for tri-band operation. More specifically, the shape and length of these parasitic elements generated different resonant modes. A similar concept was implemented in [26] by shortening the ground and feed line using a parasitic element. Next, a multiband monopole antenna utilized capacitive CPW (CCPW) feed and double square slot technique to enable a tri-band antenna operation [27, 28]. The CCPW technique is found to be useful in controlling

Table 1. Comparison of CPW antennas.

Ref.	Topology	Operating Bands [GHz]	Gain dBi	Radiation Pattern.
[14]	H-shaped Slot radiator	2.34–2.43, 3.42–4.24, 5.09–5.6	NA	XZ plane: Omnidirectional, XY plane: non-directional
[15]	CPW-fed slot antenna	1.6–1.8, 2.4–2.5, 3.3–3.7, 5.15–5.82	NA	Radiation oriented to the left of XY plane
[16]	Slot with tuning stub & split ring	1.71–2.5, 4.17–4.6, 5.725–5.825	NA	XY plane: Omnidirectional, YZ plane: non-directional
[17]	2 sleeves inside ground plane	2.38–2.85, 3.35–4.30, 5.12–5.85	3, 3.8, 4.5	XY plane: Omnidirectional, YZ plane: non-directional
[18]	2 U-shaped slot in radiating element	2.28–2.9, 3.3–3.85, 4.72–6.4	NA	Omnidirectional pattern
[19]	Meandered slots on ground plane	2.4–2.5, 3.5–10.9	1.5, 2	XZ plane: Omnidirectional, XY plane: non-directional
[20]	Elliptical slot on ground plane	0.8–0.9, 1.3–1.4, 1.6–4	NA	Unidirectional pattern
[21]	2 ladder-shaped slot on radiator	1.69–1.85, 2.2–2.96, 3.39–3.84, 5.14–7.28	NA	Omni-directional pattern
[22]	U, F & L shape slots	0.92–93, 2.44–2.46, 3.52–3.62, 5.70–6.27	−3.8, −2.8, 9.6, 9.2	Omni-directional in XZ & YZ plane
[23]	Top loading antenna	1.5–1.9, 2.51–2.62,	NA	Omni-directional in elevation plane
[24]	Parasitic element in ground plane	2.23–2.4, 3.41–3.6, 4.97–6.51	1.61, 3.39, 1.78	Omni-directional pattern
[26]	Shorted strips	0.9–0.93, 1.5–1.58, 4.97–6.51	NA	Omni-directional in XZ & YZ plane
[27]	Double square slots	1.7–2.2, 3.3–3.75, 5.05–6	2.45, 1.35 2.5	Omni-directional pattern
[28]	Interdigital capacitor	1.6–2.5, 3.3–4.3, 4.9–6.0	1.42, 1.68, 0.25	Omni-directional pattern
This work	Stacked radiating element	0.77–0.92, 1.59–1.9 2.59–2.72, 3.28–3.7	−1.26, 1.46 2.76, 1.28	Omni-directional pattern

NA (Data not available).

the fundamental frequency as well as the harmonics, but such a technique is more complex in terms of design and optimization to achieve the required frequencies. The comparison of the published literature with the proposed antenna is given in Table 1.

In this paper, we present a quad-band CPW-fed slot antenna array for LTE and WiMAX applications. To avoid design complexity, a simple approach of stacking closely-spaced radiating elements in the slot was used to obtain multiple resonant frequencies. These mutually-coupled radiating elements placed in the slots resulted in a multiband operation ranging from 0.77 to 0.92 GHz, from 1.59 to 1.9 GHz, from 2.59 to 2.72 GHz, and from 3.28 to 3.7 GHz. Its radiation pattern is observed to be omnidirectional at all center frequencies. To the best of the authors' knowledge, this is the only quad-band CPW-fed array antenna which has been designed to operate below 800 MHz. Besides being suitable for LTE applications, the design also offers a considerable amount of bandwidth and reasonable gain level for mobile terminals.

The organization of the paper is as follows. Antenna design is first explained in Section 2 followed by a parametric study presented in Section 3. Its operation explained in terms of current distribution is presented in Section 4, and the results of the antenna performance evaluation are discussed in Section 5, prior to several concluding remarks in Section 6.

2. ANTENNA CONFIGURATION

The geometry of the CPW-fed slot array and its dimensions are shown in Figure 1. The slot array has only one layer of metallization on the top of a dielectric substrate. A low cost FR-4 substrate with a dielectric constant $\varepsilon_r = 4.6$, loss tangent $\tan\delta = 0.02$ and thickness 1.6 mm is used. A 50 Ω CPW transmission line feeds the T-junction power divider leading to the array elements. For efficient transmission, the impedance of the two power divider arms must match the impedance at the junction of the CPW line feed. The impedance of the CPW transmission line can be calculated as follows [29],

$$Z_0 = \frac{30\pi}{\sqrt{\varepsilon_{eff}}} \frac{K(k')}{K(k)} \tag{1}$$

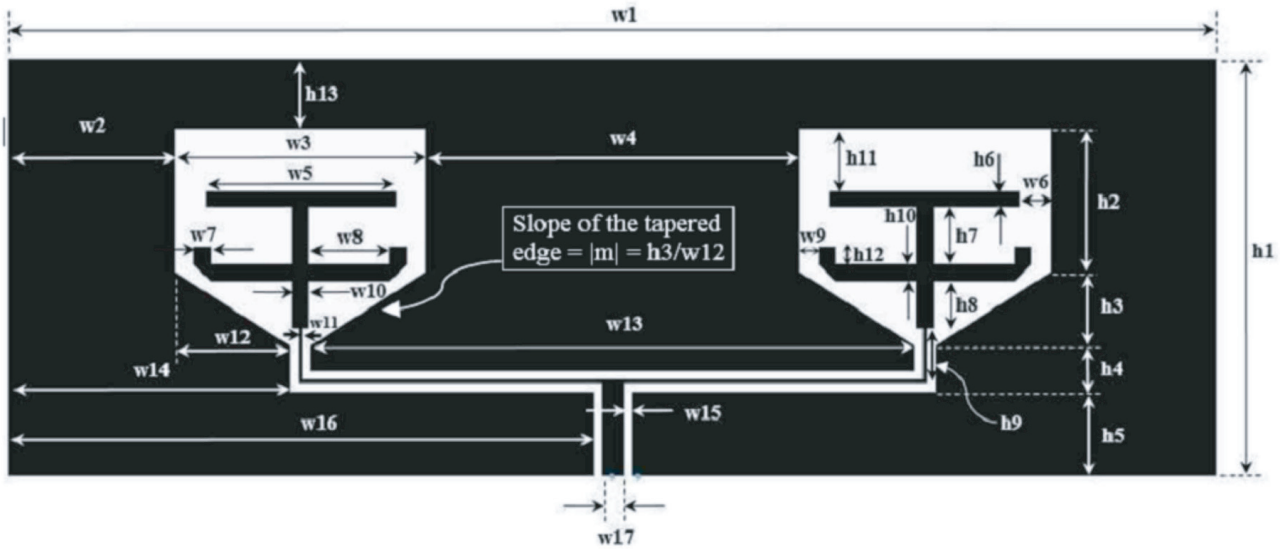

Figure 1. Geometry of CPW-fed slot antenna array. ($w_1 = 140.7$ mm, $w_2 = 19.3$ mm, $w_3 = 29.3$ mm, $w_4 = 43.54$ mm, $w_5 = 22$ mm, $w_6 = 3.64$ mm, $w_7 = 2$ mm, $w_8 = 9.42$ mm, $w_9 = 2.22$ mm, $w_{10} = 2$ mm, $w_{11} = 0.42$ mm, $w_{12} = 13.43$ mm, $w_{13} = 70.4$ mm, $w_{14} = 32.73$ mm, $w_{15} = 1$ mm, $w_{16} = 68.13$ mm, $w_{17} = 2.44$ mm, $h_1 = 48.5$ mm, $h_2 = 19.2$ mm, $h_3 = 8.6$ mm, $h_4 = 5.36$ mm, $h_5 = 9.77$ mm, $h_6 = 1.8$ mm, $h_7 = 6.58$ mm, $h_8 = 5.53$ mm, $h_9 = 6.33$ mm, $h_{10} = 2.07$ mm, $h_{11} = 9.82$ mm, $h_{12} = 2.04$ mm, $h_{13} = 5.6$ mm.)

where, $\varepsilon_{eff} = 1 + \frac{\varepsilon_{r-1}}{2}\frac{K(k')}{K(k_1)}\frac{K(k_1)}{K(k_1')}$, $k = a/b$, $k_1 = \frac{\sinh((\pi)(a)/(2h))}{\sinh((\pi)(b)/(2h))}$, $k' = \sqrt{1-k^2}$ and $K_1' = \sqrt{1-k^2}$.

The ratio of $\frac{k(k)}{k(k')}$ can be obtained as,

$$\frac{k(k)}{k(k')} = \begin{cases} \dfrac{\pi}{\ln\left(2\dfrac{1+\sqrt{k'}}{1-\sqrt{k'}}\right)} & : 0 \le k \le 0.707 \\ \dfrac{1}{\pi}\ln\left(2\dfrac{1+\sqrt{k}}{1-\sqrt{k}}\right) & : 0.707 \le k \le 1 \end{cases}$$

It can be observed that the CPW transmission line impedance depends on the strip width, feed gap and height of the substrate. The centre of the CPW line feed has a characteristic impedance of 50 Ω (which corresponds to strip width $w_{17} = 2.444$ mm and gap width $w_{15} = 1$ mm). This section is extended to the two arms of a −3 dB power divider which is 100 Ω each (corresponding to the strip width 0.42 mm and gap of 1 mm). This impedance matches the impedance of the junction of the CPW transmission line. The arms of the power divider lead to the radiating section which consists of a slot and two radiating elements. The main slot sized at $w_3 + 2h_2 + 2\sqrt{w_{12}^2 + h_3^2}$ is the key in determining the lowest resonance in the design, which in this case is approximately less than $\lambda_g/2$ at 0.8 GHz. On the other hand, the two radiating elements enable multiple frequency operation for the overall structure, where the longer driven element resonates at 1.8 GHz, and the shorter one resonates at 3 GHz when being operated independently.

When both elements are implemented at the same time, the length for the longer radiator is $2h_{12} + 2w_8 + w_{10} = 0.15\lambda_g$, and that of the shorter element is $w_5 = 0.11\lambda_g$), with a gap of ($h_7 = 0.032\lambda_g$) between them. They are optimized so that the antenna resonates at the centre frequencies of 0.8, 1.8, 2.6 and 3.45 GHz. In addition, the frequency at 2.6 GHz is obtained by optimizing the gap between the two radiating elements. To improve impedance matching at 3.45 GHz, the lower edges of the rectangular-based slot are tapered. The locations of the radiating elements and the slot are closely coupled to each other, i.e., changes in any one of them will affect the frequency associated with others. This will be further analyzed in terms of current distribution in Section 4.

3. PARAMETRIC ANALYSIS

To study the effect of different parameters on the antenna performance, the length of radiators (w_5 and $w_8 + h_{12}$), the spacing between stacked elements (h_7), and the shape and size of the slots ($w_3 + 2h_2 + 2\sqrt{w_{12}^2 + h_3^2}$) are investigated. In Figure 2, the reflection coefficient (S_{11}) is chosen as the baseline of this performance analysis.

Figure 2(a) shows the simulated S_{11} for the proposed antenna with varied h_{12}, which contributes to the length of the radiator. By increasing h_{12}, the resonances at 2.6 GHz and 3.45 GHz are lowered, whereas its operation centred at 1.8 GHz remains constant. This is due to the increase in h_{12} which is equivalent to the gap decrease between the radiating elements. The important point is that increment in h_{12} causes a shift to lower frequencies caused by the mutual coupling between the radiators. The performance of antenna is also affected by the spacing between the two radiating elements (h_7) as shown in Figure 2(b). The antenna operations in the 1.8 GHz and 2.6 GHz bands are sensitive towards mutual coupling between the two stacked radiating elements which can be controlled by varying the gap between them. There are no significant changes in performance at 0.8 GHz and 3.45 GHz due to this parameter's variation. On the other hand, parameter w_5 (length of shorter radiator) is sensitive in optimizing the antenna operation at 1.8 GHz, 2.6 GHz and 3.45 GHz.

A study of Figure 2(c) indicates that operation centred at 1.8 GHz and 2.6 GHz shifts upwards with the decrement of w_5. This is due to the shortening of the current path and resonant length due to the decreased value of w_5. The increase of parameter w_8, on the other hand, lowers the resonant frequencies in each band, see Figure 2(d). Similar to h_7 changes in resonance due to the variation of w_8 are less significant at 0.8 GHz and 1.8 GHz than 2.6 GHz and 3.45 GHz. The shape of the slot is also an important parameter for 3.45 GHz frequency band. Meanwhile, the effect of tapering the lower edges of

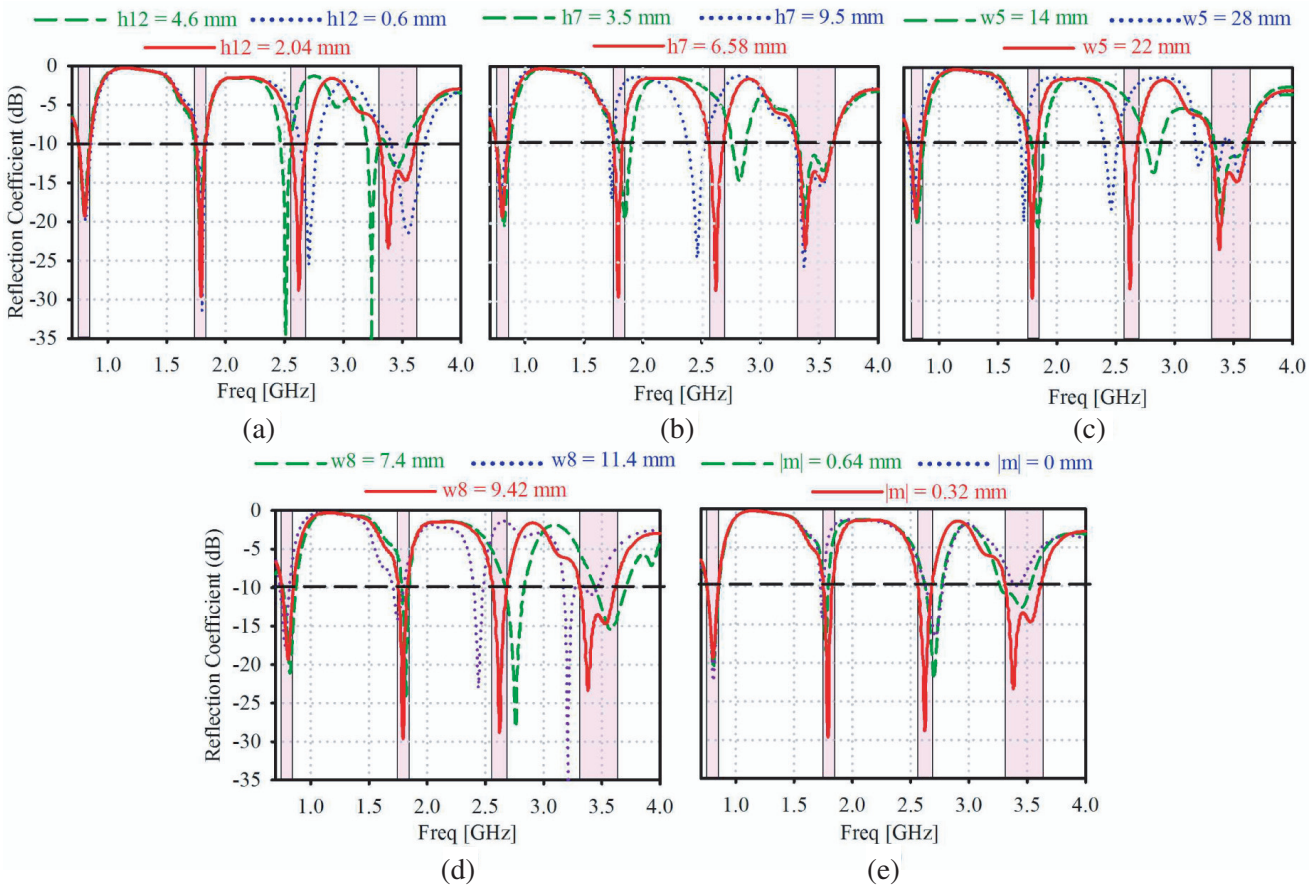

Figure 2. Parametric study (a) length of radiator (h_{12}), (b) spacing between stacked elements (h_7), (c) length of radiator (w_5), (d) length of radiator (w_8) and (e) slope of tapered edge of slot $\mid m \mid$.

the rectangular-based slot to improve matching is shown in Figure 2(e). The initial rectangular-shaped slot which results in a poor matching around 3.45 GHz is improved by changing the slope of the lower slot edge. It is also observed that this change does not affect the resonant frequency at 0.8 GHz due to the maintenance of the overall slot size dimensioned at $(w_3 + 2h_2 + 2\sqrt{w_{12}^2 + h_3^2})$. From the parametric analysis, it can be summarized that the antenna operation in all four bands is achieved by optimizing the size and length of the radiating elements, along with spacing between them and the shape of the slot. Despite the antenna multiband characteristics which are enabled by stacking of multiple resonators and their mutual coupling, the proposed design offers parameter which enables different resonances to be tuned independently.

4. CURRENT DISTRIBUTION

Figure 3 shows the current distribution at each operating frequency. As discussed in Section 2, the radiating elements in the overall antenna structure and the slots are closely spaced so are mutually coupled. The modification of the surface currents due to physical changes on any one of them can affect the current distribution on the remaining elements. The current distribution for lower resonance at 0.8 GHz shown in Figure 3(a) indicates high intensities around the edges of the slots. This implies that the size of the slot determines the lowest operating frequency for the proposed structure. It is also the main reason that the change of other parameters besides this does not affect the lower resonance at 0.8 GHz from Figure 2. Meanwhile, the current distributions at 1.8 and 2.6 GHz are illustrated in Figures 3(b) and (c), respectively. As the two radiating elements are closely coupled to each other, any changes to any element will significantly affect their current intensities and these two resonant

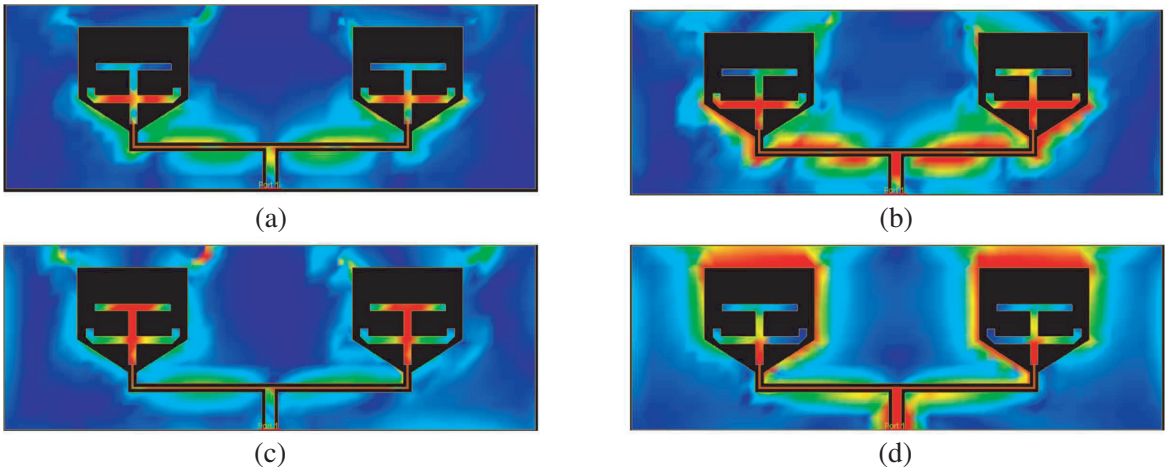

Figure 3. Current distributions at (a) 0.8 GHz, (b) 1.8 GHz, (c) 2.6 GHz, (d) 3.45 GHz.

frequencies simultaneously, as presented in Figure 2. Finally, the current distribution at 3.45 GHz is shown in Figure 3(d). A high intensity can be observed on the longer radiating element and the tapered edge of the slot. This is due to the role of the tapered edges of the slot in improving impedance matching at 3.45 GHz, in agreement with the finding from Figure 2(d).

5. EXPERIMENTAL RESULTS

Upon the completion of the optimization process, the proposed array antenna has been fabricated as shown in Figure 4. The antenna prototype is fabricated on an FR-4 substrate with a total size of $140.7 \times 48.5 \times 1.6\,\text{mm}^3$.

Comparison of the simulated and measured antenna S_{11} in Figure 5 indicates a good agreement,

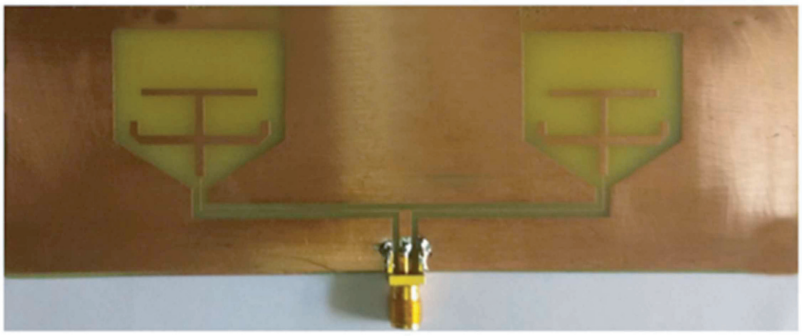

Figure 4. Prototype of proposed antenna.

Table 2. Simulated and measured gain of the proposed antenna.

Frequency	Simulated Gain (dBi)	Measured Gain (dBi)
0.80 GHz	−1.26	−1.3
1.80 GHz	1.46	1.51
2.60 GHz	2.76	2.45
3.45 GHz	1.28	1.35

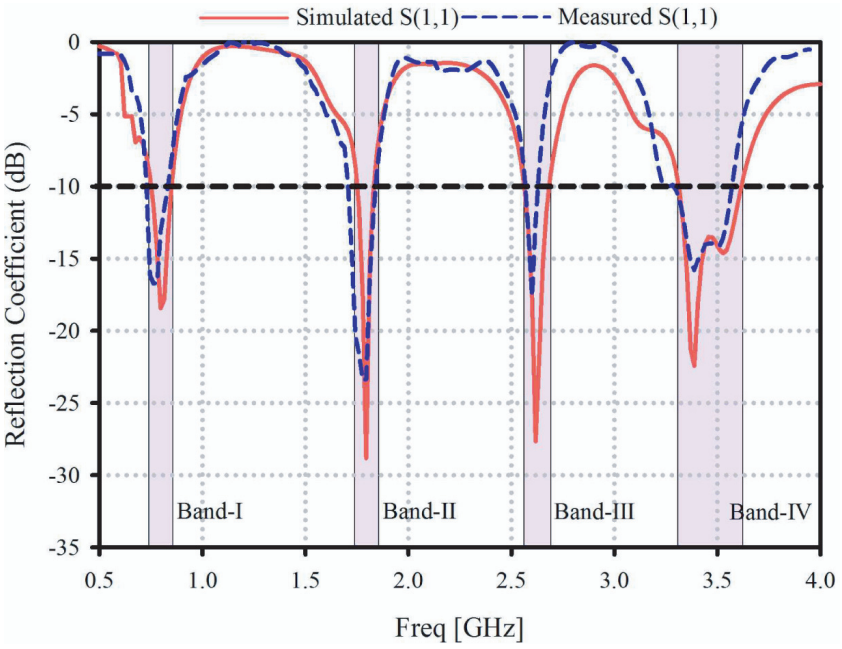

Figure 5. Simulated and measured reflection coefficient of the proposed antenna.

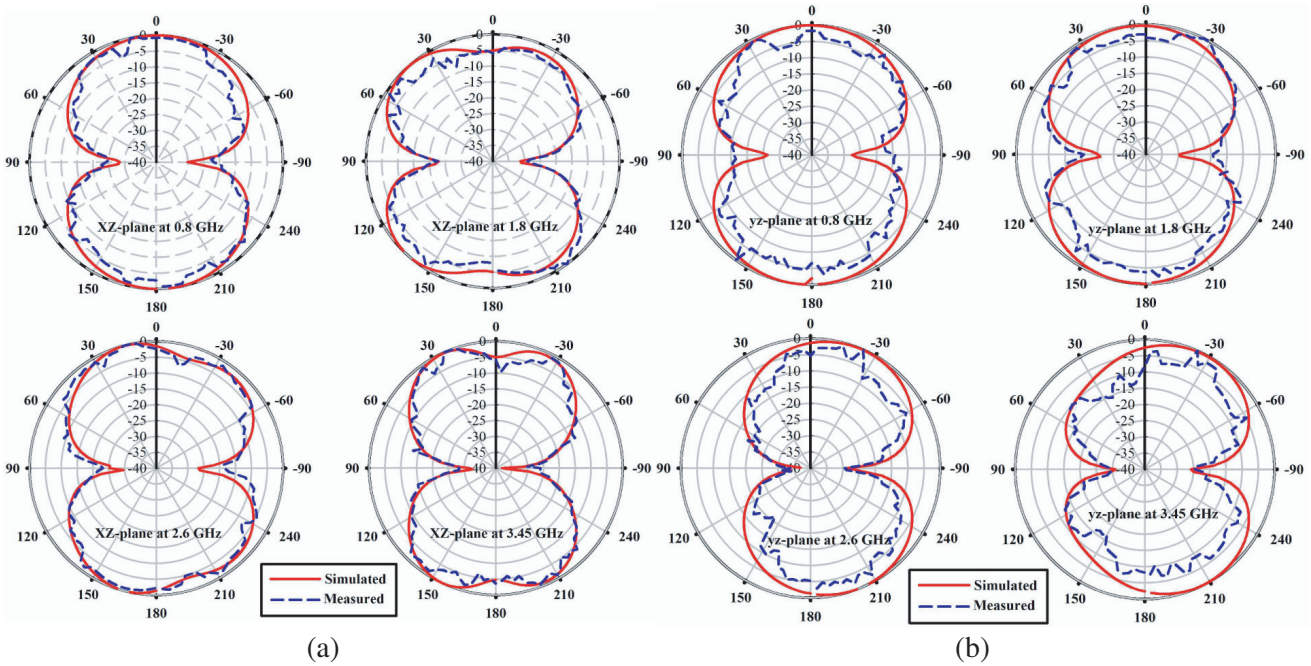

Figure 6. Electric field radiation patterns in (a) xz-plane, (b) yz-plane.

with some slight discrepancy which can be attributed to soldering imperfection and fabrication tolerance. Measurements validate that the bandwidth in Band-I is 17.75% centred at 0.845 (from 0.77–0.92) GHz which enables its application in bands 5, 6, 18, 19 and 20 for LTE. Meanwhile, the bandwidth obtained for Band-II is 17.76% centred at 1.745 GHz (operating from 1.59 to 1.9 GHz), covering operation in the LTE bands 3 and 9. Band-III operation is centred at 2.655 GHz from 2.59 to 2.72 GHz, indicating a bandwidth of 4.9%. Finally, the antenna operation in Band-IV is between 3.28 and 3.7 GHz, with a 12% bandwidth centred at 3.49 GHz. This enables the antenna to be applied to LTE band 22 and WiMAX.

The radiation patterns at the xz-plane and yz-plane at each resonant frequency are illustrated in Figures 6(a) and 6(b), respectively. Their patterns in both planes are omnidirectional at all resonant frequencies, with good agreements between simulations and measurements. Note that the proposed array antenna has strong electric field projection in the xz-plane as compared to yz-plane at 0.8 GHz, 1.8 GHz and 3.45 GHz, while they are similar at 2.6 GHz in both planes. Table 2 shows the measured and simulated peak gains at each centre frequency. The small value of the peak gain at 0.8 GHz is due to the relatively small electrical length of the slot perimeter $(w_3 + 2h_2 + 2\sqrt{w_{12}^2 + h_3^2}) = 97$ mm which is less than $\lambda_g/2$ at 0.8 GHz. Besides that, the relatively large bandwidth in this band also contributes to the lower gains.

6. CONCLUSION

A quad-band CPW-fed slot antenna array for LTE and WiMAX applications is designed. The proposed antenna utilizes a simple stacking method of closely-spaced radiating elements in a slot etched on its structure to enable its multiband behaviour. Measurement of this CPW-fed structure indicates operation in four frequency bands centred at 0.845 (from 0.77 to 0.92 GHz), 1.745 (from 1.59 to 1.9 GHz), 2.655 (2.59 to 2.72 GHz) and 3.49 GHz (from 3.28 to 3.7 GHz). This corresponds to the bandwidths of 17.75% in Band-I, 17.76% in Band-II, 4.9% in Band-III and 12% in Band-IV. Simulated and measured radiation patterns for this structure agree well and indicate an omnidirectional behavior, which is suitable for its application in mobile devices, with gains up to 2.45 dBi. The proposed antenna can be potentially applied to operation in the LTE bands 3, 5, 6, 9, 18, 19, 20 and 22 and WiMAX.

REFERENCES

1. Holma, H., A. Toskala, K. Ranta-Aho, and J. Pirskanen, "High-speed packet access evolution in 3 gpp release 7 [topics in radio communications]," *IEEE Communications Magazine*, Vol. 45, No. 12, 29–35, 2007.
2. Mun, B., F. J. Harackiewicz, B. Kim, H. Wi, J. Lee, M. J. Park, and B. Lee, "New configuration of handset MIMO antenna for LTE 700 band applications," *International Journal of Antennas and Propagation*, 2013.
3. Schaubert, D. H., "A review of some microstrip antenna characteristics," *Microstrip Antennas*, 59–67, 1995.
4. Soliman, E. A., S. Brebels, G. Vandenbosch, and E. Beyne, "X-band brick wall antenna fed by CPW," *Electronics Letters*, Vol. 34, No. 9, 836–838, 1998.
5. Miao, M., B. L. Ooi, and P. S. Kooi, "Broadband CPW-fed wide slot antenna," *Microwave and Optical Technology Letters*, Vol. 25, No. 3, 206–211, 2000.
6. Liu, H. C., T. S. Horng, and N. G. Alexopoulos, "Radiation of printed antennas with a coplanar waveguide feed," *IEEE Transactions on Antennas and Propagation*, Vol. 43, No. 10, 1143–1148, 1995.
7. Sayem, A. and M. Ali, "Characteristics of a microstrip-fed miniature printed Hilbert slot antenna," *Progress In Electromagnetics Research*, Vol. 56, 1–18, 2006.
8. Eldek, A. A., A. Z. Elsherbeni, and C. E. Smith, "Dual-wideband square slot antenna with a U-shaped printed tuning stub for personal wireless communication systems," *Progress In Electromagnetics Research*, Vol. 53, 319–333, 2005.
9. Sadat, S. and S. D. S. Javan, "Design of a microstrip square-ring slot antenna filled by an H-shape slot for UWB applications," *2007 IEEE Antennas and Propagation Society International Symposium*, 705–708, IEEE, 2007.
10. Huang, J. F., "A simple model of designing CPW-fed slot antenna," *2nd International Conference on Microwave and Millimeter Wave Technology, ICMMT*, 383–386, IEEE, 2000.
11. Bhobe, A. U., C. L. Holloway, M. Piket-May, and R. Hall, "Coplanar waveguide fed wideband slot antenna," *Electronics Letters*, Vol. 36, No. 16, 1340–1342, 2000.

12. Waterhouse, R. B. and D. Novak, "Small folded CPW fed slot antennas," *2006 IEEE Antennas and Propagation Society International Symposium*, 2599–2602, IEEE, 2006.
13. Saed, M. A., "Reconfigurable broadband microstrip antenna fed by a coplanar waveguide," *Progress In Electromagnetics Research*, Vol. 55, 227–239, 2005.
14. Kumar, A., "A compact H-shaped slot triple-band microstrip antenna for WLAN and WiMAX applications," *2016 IEEE Annual India Conference (INDICON)*, 1–4, IEEE, 2016.
15. Avila, D. R., S. P. García, Y. P. Marrero, A. S. de Vera, F. M. Rizo, J. V. L. Sanz, and A. T. Puente, "Multiband CPW-fed slot antennas," *10th European Conference on Antennas and Propagation (EuCAP)*, 1–4, IEEE, 2016.
16. Joseph, S., B. Paul, S. Mridula, and P. Mohanan, "CPW-fed compact multiband antennas using circular monopole with hexagonal slot," *Fifth International Conference on Advances in Computing and Communications (ICACC)*, 287–290, IEEE, 2015.
17. Wang, Y., Q. Y. Zhang, and Q. X. Chu, "Triple-band monopole antenna with dual-sleeves inside the ground plane," *Asia Pacific Microwave Conference, APMC 2009*, 1980–1983, IEEE, 2009.
18. Cai, L. Y., G. Zeng, and H. C. Yang, "Compact triple band antenna for Bluetooth/WiMAX/WLAN applications," *International Symposium on Signals Systems and Electronics (ISSSE)*, Vol. 2, 1–4, IEEE, 2010.
19. Bhaskar, S., R. S. Brar, and A. K. Singh, "Compact planar rectangular monopole antenna for Bluetooth and UWB applications," *International Conference on Electrical, Computer and Electronics Engineering (UPCON), 2016 IEEE Uttar Pradesh Section*, 138–141, IEEE, 2016.
20. Lin, T., L. Song, S. Liu, Y. Wang, and Z. Li, "Novel conformal Vivaldi antenna fed by CPW," *2016 IEEE International Conference on Microwave and Millimeter Wave Technology (ICMMT)*, Vol. 2, 725–727, IEEE, 2016.
21. Wang, J. and Y. Yang, "A compact four bands microstrip patch antenna with coplanar waveguide feed," *3rd Asia-Pacific Conference on Antennas and Propagation (APCAP)*, 33–36, IEEE, Vancouver, 2014.
22. Li, H., Y. Zhou, X. Mou, Z. Ji, H. Yu, and L. Wang, "Miniature four-band CPW-fed antenna for RFID/WiMAX/WLAN applications," *IEEE Antennas and Wireless Propagation Letters*, Vol. 13, 1684–1688, 2014.
23. Soler, J., F. J. Gonzalez, C. Puente, and J. Anguera, "Advances in loading techniques to design multifrequency monopole antennas," *Microwave and Optical Technology Letters*, Vol. 41, No. 6, 434–437, 2004.
24. Verma, S. and P. Kumar, "Compact triple-band antenna for WiMAX and WLAN applications," *Electronics Letters*, Vol. 50, No. 7, 484–486, 2014.
25. Wang, C. J. and K. L. Hsiao, "CPW-fed monopole antenna for multiple system integration," *IEEE Transactions on Antennas and Propagation*, Vol. 62, No. 2, 1007–1011, 2014.
26. Zahraoui, I., J. Zbitou, A. Errkik, E. Abdelmounim, A. Tajmouati, and M. Latrach, "Novel low cost compact printed antenna CPW-fed for GSM, GPS and PCS applications," *Third International Workshop on RFID and Adaptive Wireless Sensor Networks (RAWSN)*, 48–51, IEEE, 2015.
27. Singsura, P., P. Chomtong, S. Meesomklin, and P. Akkaraekthalin, "A multiband monopole antenna with double square slots and capacitive CPW feed for LTE, WiMAX and WLAN systems," *12th International Conference on Electrical Engineering/Electronics, Computer, Telecommunications and Information Technology (ECTI-CON)*, 1–5, IEEE, 2015.
28. Chomtong, P. and P. Akkaraekthalin, "A multiband slot CPW antenna using capacitive feed and interdigital capacitor for GSM, WiMAX and WLAN systems," *Asia-Pacific Conference on Communications (APCC)*, 446–449, IEEE, 2014.
29. Wadell, B. C., *Transmission Line Design Handbook*, Artech House, 1991.